

# Analysis and Prevention of Dent Defects Formed during Strip Casting of Twin-Induced Plasticity Steels

MANJIN HA, WAN-SOO KIM, HEE-KYUNG MOON, BYEONG-JOO LEE,  
and SUNGHAK LEE

Rapid-solidification experiments were conducted for understanding dent defects formed during strip casting of twin-induced plasticity (TWIP) steels. The rapid-solidification experiments reproduced the dent defects formed on these steels, which were generally located at valleys of the shot-blasted roughness on the substrate. The rapid-solidification experiment results reveal that the number of dips, the Mn content of the steel, and the surface roughness of the substrate affect the depth and size of dents formed on the solidified-shell surfaces, while the composition of the atmosphere gases and the carbon content of the steel are not factors. The formation of dents was attributed to the entrapment of gases inside the roughness valleys of the substrate surface and their volume expansion due to the temperature of the steel melt and the latent heat. The dents could be prevented when the thermal expansion of gases was suppressed by making longitudinal grooves on the substrate surface, which allowed the entrapped gases to escape. Sound solidified shells were obtained by optimizing the width and depth of the longitudinal grooves and by controlling the shot-blasting conditions.

DOI: 10.1007/s11661-008-9496-3

© The Minerals, Metals & Materials Society and ASM International 2008

## I. INTRODUCTION

THE rapid solidification of strip casting, compared to conventional continuous casting, can be exploited for reducing microsegregation, extending solute solubility limit, and refining the solidification structure. It is also an environmentally conscious production process that can possibly reduce manufacturing costs, labor, and energy since the hot-rolling step can be omitted. Thus, studies on strip casting have been intensively undertaken to capitalize on these advantages. Production facilities to commercialize STS 304 stainless steels and other steels have been completed, and commissioning of the steel-strip production is in progress.<sup>[1-7]</sup> Since strip casting can omit the hot-rolling process, it is also especially suited for the production of steels that are problematic during hot rolling and can open the opportunity to develop new advanced steels.

Twin-induced plasticity (TWIP) steels are promising steels with a high potential for automotive applications, since they have dramatically improved elongation, high strength, and high formability, according to the twin transformation behavior during the forming processes.<sup>[8-10]</sup> However, they face many problems arising

from hot rolling, such as decreased production yield by grain-boundary oxidization during reheating, generation of microscabs on the surface by selective oxidization due to excessive containment of Al and Mn in the steel,<sup>[11,12]</sup> and crack initiation during hot rolling of slabs. Therefore, these problems are expected to be solved by applying the strip-casting process to TWIP steels, which eliminates the hot-rolling step.

One of the defects found on the surface of cast strips of TWIP steels are gas pockets (Figure 1). These are also called "dent" defects and are 0.1- to 0.5-mm deep and 0.3 to 1.5 mm in diameter. These defects are "dented" on the cast-strip surface, and surface cracks can be initiated along these dents. Dent defects are present only on the surface of cast strips, whereas pinhole defects are not present beneath the surface. Since dent defects can deteriorate mechanical properties and cause surface defects of the steel strips, their prevention or reduction is an important consideration. These dent defects observed in the strip-casting process have not been reported previously.

The shape of the dent in Figure 1 suggests that these defects apparently form due to gases present between the solidified shell and the roll. Air pockets have been observed on the surface of ribbons formed by melt spinning,<sup>[13]</sup> and their formation has been explained as due to the entrapment of air between the ribbon and the roll, as the air and roll move together during roll revolution.<sup>[13,14]</sup> This phenomenon becomes more severe at lower casting speeds and high steel-melt temperatures due to the air pockets becoming coarse as a result of thermal expansion of the entrapped gases.<sup>[14]</sup>

The present study aims to understand the mechanism of formation of dent defects found on the surface of TWIP steels made by strip casting and to provide mitigating solutions. An experimental apparatus for

---

MANJIN HA and WAN-SOO KIM, Principal Researchers, and HEE-KYUNG MOON, Senior Principal Researcher, are with the POSTRIP R&E Project Department, Technical Research Laboratories, POSCO, Pohang, 790-785 Korea. BYEONG-JOO LEE, Professor, is with the Center for Advanced Aerospace Materials, Pohang University of Science and Technology. SUNGHAK LEE is Professor, Center for Advanced Aerospace Materials, and the Department of Materials Science and Engineering, Pohang University of Science and Technology, Pohang, 790-784 Korea. Contact e-mail: shlee@postech.ac.kr

Manuscript submitted May 20, 2007.

Article published online March 26, 2008

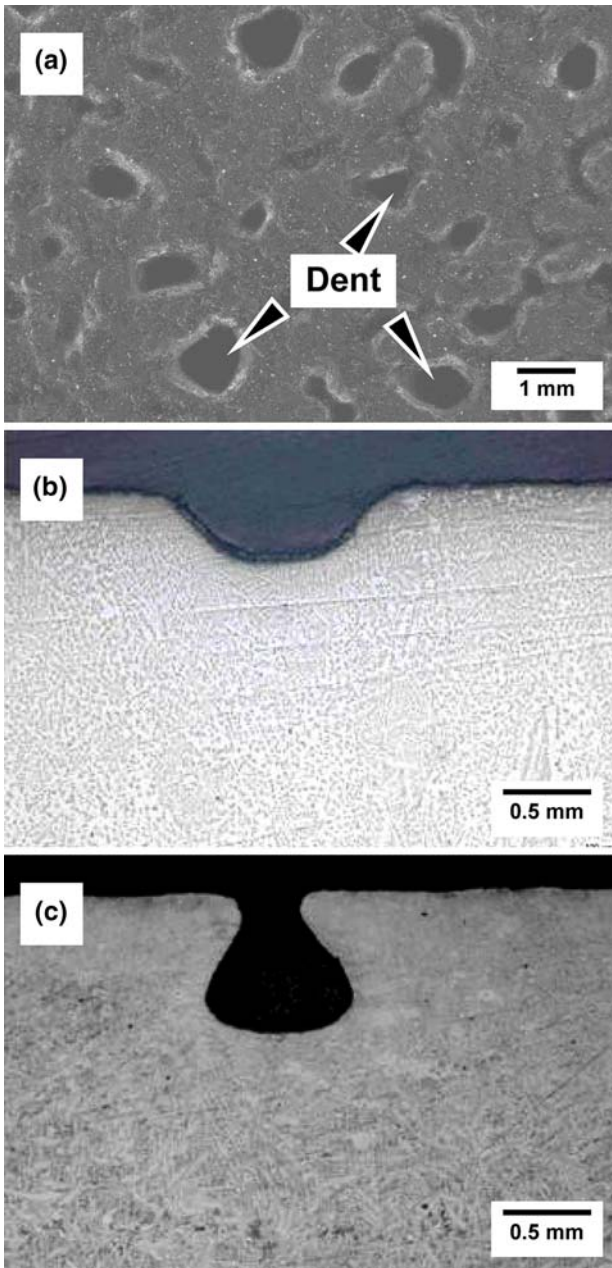


Fig. 1—Optical micrographs of the TWIP-steel cast strip produced by a twin roll strip caster, showing (a) dent defects of the surface and (b) and (c) cross-sectional shapes of dent defects.

simulating a strip caster was manufactured, and the mechanism of formation of dent defects was investigated by observing their behavior as a function of composition, atmosphere gas, substrate-surface roughness, and oxide layer of the substrate surface.

## II. EXPERIMENTAL

Figure 2 illustrates schematically a rapid-solidification apparatus for simulating a strip caster. The procedure involved forming a solidified shell when melting the steel in the 100-kg induction furnace and then immersing the substrate into the steel melt for a short period of time.

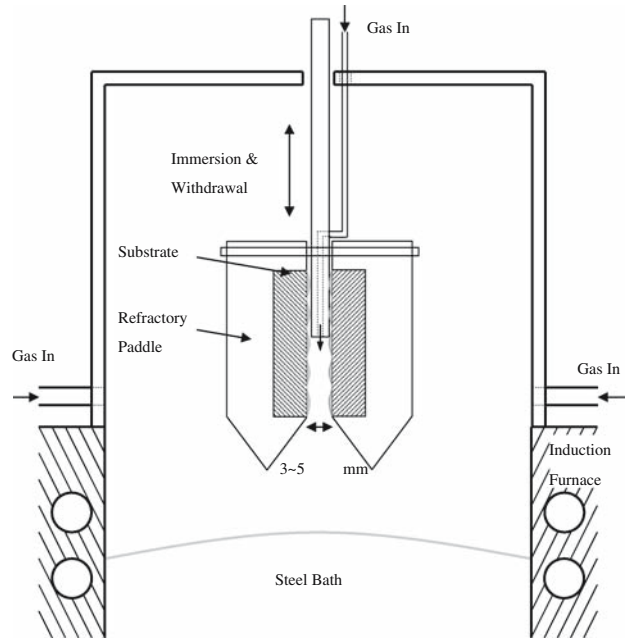


Fig. 2—Schematic diagram of a rapid-solidification apparatus for simulating a strip caster.

The contacting time of the substrate with the steel melt was 0.5 to 1.0 seconds, and the immersion depth was 50 to 100 mm. The substrate used was made by electroplating 2-mm-thick nickel on a 20-mm-thick, 100-mm-wide, and 200-mm-long copper plate, followed by shot blasting to an average roughness ( $R_a$ ) of  $20 \mu\text{m}$  with a standard deviation of 1.2 to  $1.5 \mu\text{m}$ . Figure 3 shows the shot-blasted surface roughness and the substrate surface after dipping. The dipped substrate surface turned black due to the formation of an oxide layer, whereas a brown powder layer was formed in the nondipped region.

To verify the reliability of the simulation test, the secondary dendrite arm spacing (SDAS) inside the solidified-shell microstructure of an STS 304 stainless steel was measured. The measured SDAS of 4 to  $5 \mu\text{m}$  in the surface region and 6 to  $8 \mu\text{m}$  in the interior region is similar to that observed in an actual strip-casting process. Some cracks initiated, or inhomogeneous solidification occurred on the surface of the solidified shell, since this was constrained at the edge of the substrate when dipping the copper/nickel substrate into the steel melt. Thus, silica refractory paddles were fabricated, and the substrate was placed inside the paddles. Two paddles were placed face to face with a gap of 3 to 5 mm between them. This setup enabled the comparison of the formation behavior of the solidified shell in two substrates with different conditions. Since the steel melt was introduced only through the narrow gap, slag or impurities floating on the melt surface were not mixed into the solidified-shell surface. As a result, sound and reproducible solidified shells could be fabricated with this experimental apparatus. The solidified-shell specimens were approximately 3- to 5-mm thick, 100-mm wide, and 50- to 80-mm high.

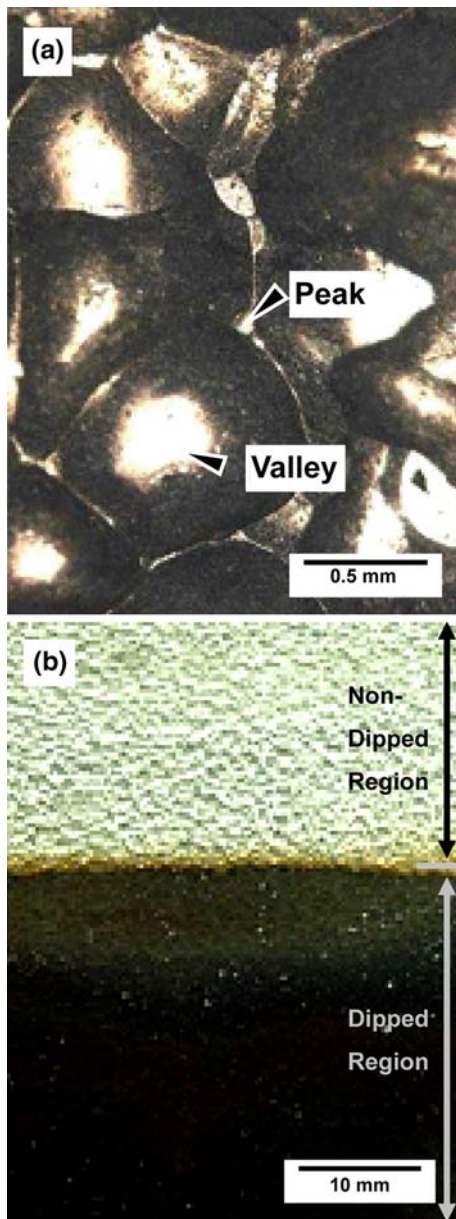


Fig. 3—Photographs of the surface of the substrate, showing (a) the shot-blasted surface roughness and (b) the difference between the nondipped (upper part) and dipped (lower part) regions.

In order to maintain the atmosphere gas inside the induction furnace, a gas chamber was created in the upper part of the furnace, which was then sealed. The gas was introduced into the chamber to lower the oxygen concentration to below 0.1 pct. The gas was introduced into the gap between the two facing substrates to strictly control the atmosphere at the regions where the steel melt and the substrate contacted. Various gases, such as nitrogen, argon, and 1 pct  $O_2$ -99 pct  $N_2$  mixed gas were introduced between the substrates to study the effect of the local environment on the formation of dent defects.

The basic chemical composition of the TWIP steels used as the steel melt was 0.5C-25Mn-1.5Al-0.1Si in wt pct. By varying the C content from 0 to 0.5 wt pct, Mn

from 0 to 25 wt pct, and Al from 0 to 1.5 wt pct, the effects of the chemical composition on the formation of the dent defects were studied. The oxygen, nitrogen, and hydrogen inside the steel were controlled between 0 to 10 ppm, 100 to 200 ppm, and 5 to 15 ppm, respectively.

To examine the effect of substrate roughness on dent formation, the shot-blasting conditions were varied to create average roughness ( $R_a$ ) values of 5.5, 8, and 20  $\mu\text{m}$ . The roughness was measured with a two-dimensional roughness tester (model SJ-400, Mitutoyo Company, Kawasaki, Japan) with a cutoff length of 2.5 mm and a measured length of 12.5 mm.

The wetting angle between the substrate and steel melt was measured by the sessile drop method to confirm the wettability and reactivity between the oxides formed on the substrate surface and the TWIP-steel melt.<sup>[15-17]</sup> A bar-shaped TWIP-steel specimen 4 mm in diameter and 4.5 mm in height was placed on a 98 pct alumina substrate or a Mn oxide (MnO) substrate, which was then heated to 1550  $^\circ\text{C}$  to melt the TWIP-steel bar specimen. Graphite heating elements were used in the furnace. A vacuum was maintained at temperatures below 1100  $^\circ\text{C}$ , while an argon-gas atmosphere was maintained at temperatures higher than 1100  $^\circ\text{C}$ . After the bar specimen melted, the contact shape of the steel melt and the substrate was photographed at intervals of several seconds with a camera installed outside the furnace. The wetting angle reported was for the drop shape that sustained after 30 minutes following melting. The cooled specimens were examined with a scanning electron microscope (SEM) to study the reaction products formed at the interface between the substrate and the TWIP steel.

### III. RESULTS

#### A. Effects of Number of Dipping

Photographs of the surface of the solidified shells are shown in Figures 4(a) through (d) in order of the number of dips, and the depth of the dent defect as a function of number of dips is plotted in Figure 5. Dent defects are not seen to occur in the solidified shell formed after the first dip (Figure 4(a)) but start to show in the second dip (Figure 4(b)) and grow with an increase in the number of dips (Figures 4(c) and (d)). Surface cracks form as the dents deepen, as shown with an arrow marked in Figures 4(c) and (d). The dent reaches a maximum depth of 250  $\mu\text{m}$  with an increasing number of dippings (Figure 5), while the dent diameter ranges from 0.5 to 1.5 mm. The dent shape and depth are similar to that obtained in actual strip casting. In the subsequent experiments, the fourth dipping was used as the standard for comparison with other conditions.

As noted earlier, the Ni substrate surface turned black after the first dipping due to the formation of an oxide layer (Figure 3), which was analyzed by X-ray diffraction to be MnO (Figure 6). Energy dispersive spectroscopy (EDS) was conducted on the substrate and the cross section of the solidified shell to study the thickness of the oxide layer on the substrate surface as a function

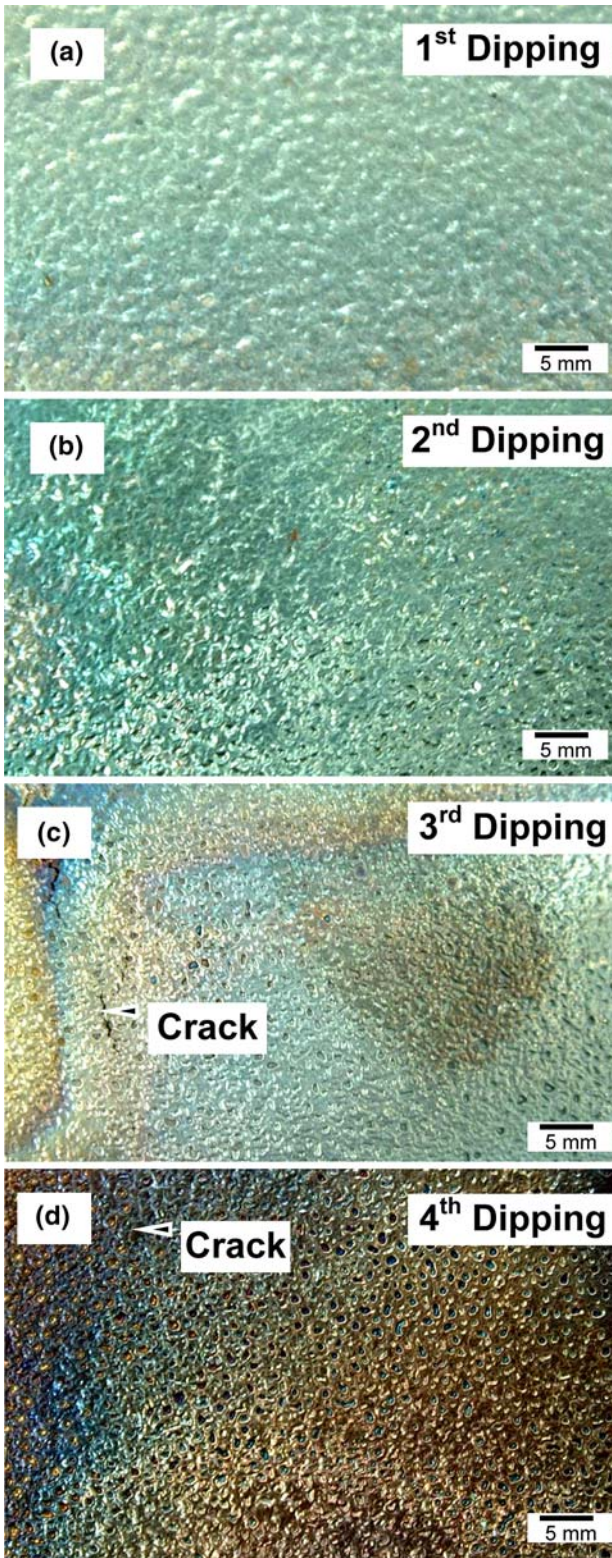


Fig. 4—Photographs of the surface of solidified shells after the (a) first, (b) second, (c) third, and (d) fourth dipping.

of the number of dips (Figures 7(a) through (f)). After the first dip, the Mn oxide layer on the substrate surface was 5  $\mu\text{m}$  in maximum thickness and was discontinuous on the Ni substrate (Figures 7(a) through (c)). After the

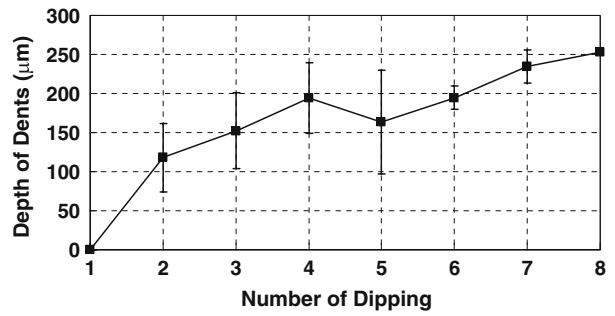


Fig. 5—Depth of dent defects as a function of number of dips.

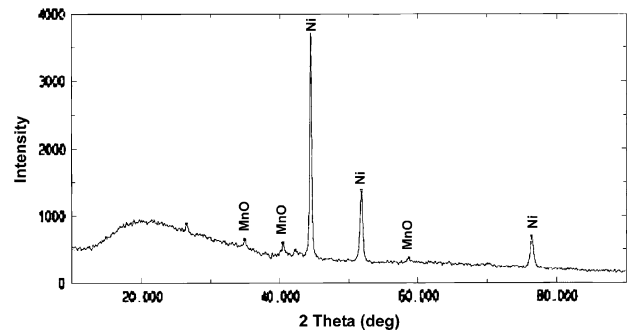


Fig. 6—X-ray diffraction spectrum of the oxide layer formed on the nickel substrate surface.

fourth dip, the Mn oxide layer was approximately 25- $\mu\text{m}$  thick and covered the Ni substrate continuously (Figures 7(d) through (f)). The oxide layer had fallen off from the substrate surface at locations corresponding to the roughness peak of the substrate and became stuck to the solidified-shell surface (arrow marked in Figure 7(e)).

After the first dip, the substrate temperature was approximately 200  $^{\circ}\text{C}$ . After cooling the substrate with argon gas, the substrate with oxide layer was dipped again at room temperature, and the result was the formation of dents. This experiment indicated that the temperature increase of the substrate after the redipping did not influence the formation of dents. When the substrate was dipped again after the oxide layer was removed from the substrate surface in a 50 pct HCl solution, washed in alcohol, and dried, the dents did not occur. Figures 8(a) through (d) show a substrate containing both the first- and the fourth-dipped regions by dipping the substrate three times to a depth of 50 mm, and then once to a depth of 80 mm. Dents were not observed in the region that first contacted the steel melt, and the roughness shape of the solidified shell was different from that of the substrate surface (Figure 8(b)). In the fourth-dipped region, the roughness shape of the solidified-shell surface was a replica of the substrate surface, and dents were formed at roughness peaks of the solidified-shell surface (Figure 8(d)). This experiment showed that dent formation was related to the degree to which the steel melt replicated the substrate surface roughness, as well as the formation behavior of the oxide layers on the substrate surface.

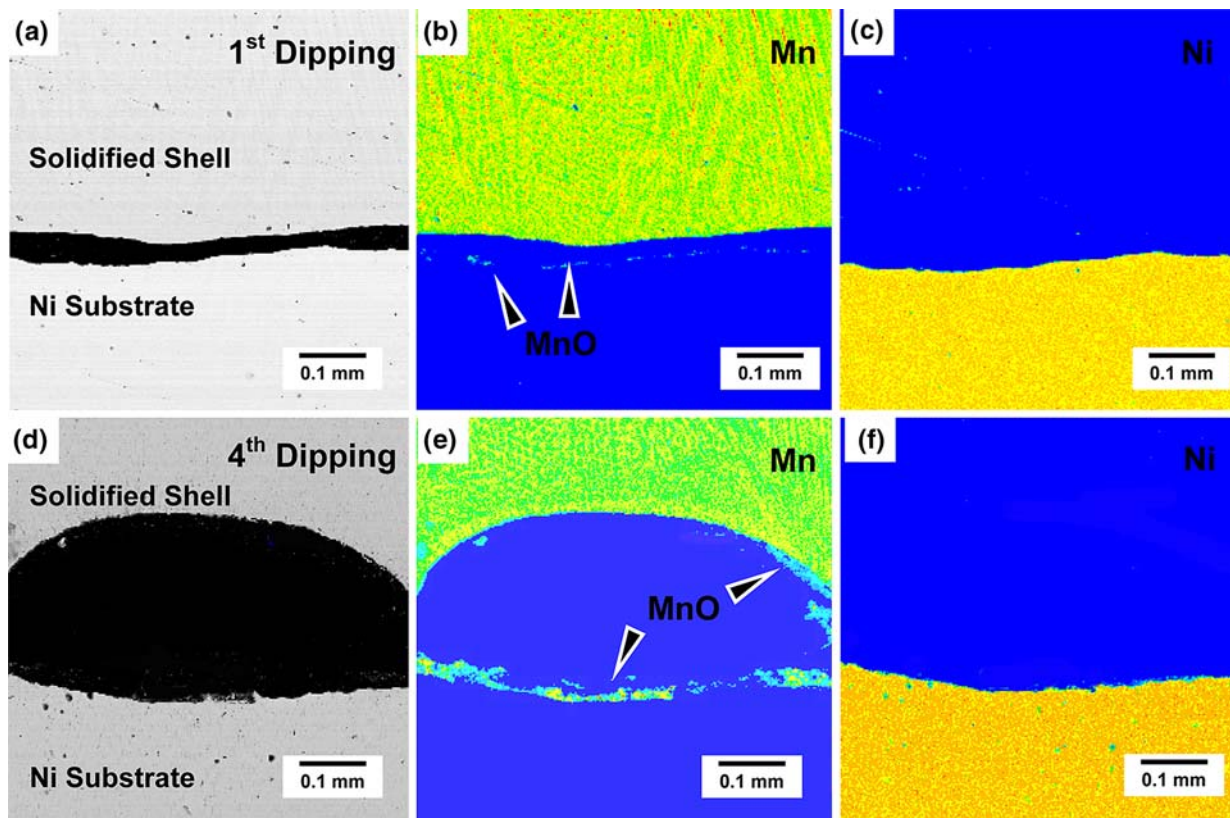


Fig. 7—(a) BEI of the solidified shell and nickel substrate after the first dip and (b) and (c) EDS mapping of Mn and Ni. (d) through (f) BEI image and EDS map results of the solidified shell and nickel substrate after the fourth dip.

### B. Wetting Angles of TWIP-Steel Melt

Figures 9(a) through (e) show the figures of wetting angles of the steel melt on the alumina and MnO substrates following the use of the sessile-drop experiment,<sup>[15–17]</sup> and the wetting angles are measured. To verify the reliability of the wetting-angle measurement, the wetting angle of a plain carbon steel on the alumina substrate was determined, which showed an angle of 103 deg (Figure 9(a)), which is similar to the wetting angle of 105 deg measured for 0.4 pct C steel on 98 pct alumina substrate by Nakashima *et al.*<sup>[16]</sup> The wetting angle measured for the Al-added TWIP steel on the alumina substrate is 95 deg, while that for the non-Al-added TWIP steel is 78 deg (Figures 9(b) and (c)). These measurements imply that the TWIP-steel melt has relatively good wettability on the alumina substrate. To study how the MnO layer formed on the substrate surface affects the wettability of TWIP steels, an MnO substrate was used to measure the wetting angles with various steels, and the results are shown in Figures 9(d) and (e). The wetting angle of the Al-added TWIP steel is 57 deg, and that of the non-Al-added TWIP steel is 67 deg (Figures 9(d) and (e)). These are lower than the wetting angles obtained with the alumina substrate (Figures 9(b) and (c)), indicating better wettability of the TWIP- steel melt with MnO.

Figures 10(a) through (c) show reaction products formed at the interface of the MnO substrate and

TWIP-steel melt. Various reaction products were observed at or around interface in both the Al-added and the non-Al-added TWIP steels. Table I shows the composition of the reaction products obtained by EDS analysis of the areas marked A through F.  $\text{Al}_2\text{MnO}_4$ , (Mn,Al) oxides, and (Mn,Al,Fe) oxides are observed at the interface of the Al-added TWIP steel and the MnO substrate (Figure 10(a), and areas A, B, and C of Table I), and  $\text{Al}_2\text{MnO}_4$  and (Mn,Si,Al) oxides are observed inside the TWIP steel near the interface (Figure 10(b) and areas D and E of Table I). (Mn,Al,Si,Fe) oxides are found in the non-Al-added TWIP steel (Figure 10(c) and area F of Table I). These data imply that various reaction products that formed at the interface of the MnO and the TWIP-steel melt enhanced the wettability of the MnO substrate and the TWIP-steel melt. No pores formed due to the reactions at the TWIP- steel/MnO interfaces.

### C. Effects of Atmosphere Gas

Atmosphere gases remain between the steel melt and substrate in the strip-casting process, which affect the thermal transfer and wetting behavior. This is particularly true in strip casting of STS 304 steel, where the wetting behavior is greatly affected by a variety of atmosphere gases.<sup>[18]</sup> The rapid-solidification test was conducted by varying the atmosphere gas, and the

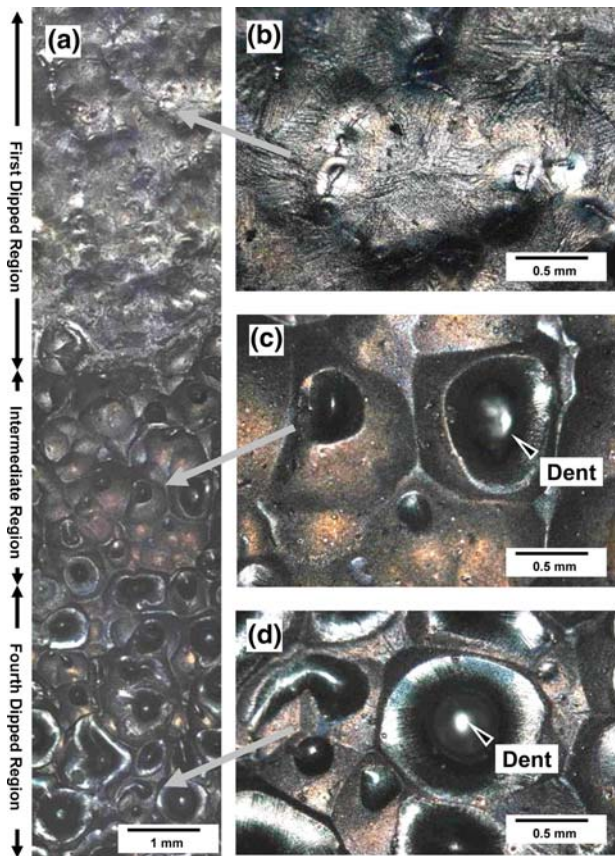


Fig. 8—(a) Optical micrograph of the surface of the solidified shell after the fourth dip, showing both the first and fourth dipped regions. (b) through (d) Higher-magnification optical micrographs of the first, intermediate, and fourth dipped regions, respectively, as indicated by arrows.

results are provided in Figure 11. The depth of dents increased with increasing number of dips, and increasing trends were similar irrespective of the atmosphere gas used. This observation indicated that the effect of atmosphere gases on dent formation behavior is negligible.

#### D. Effects of Substrate Surface Roughness

Figures 12(a) through (c) show photographs of the surface of the solidified shells after the rapid-solidification tests as the average surface roughness of the substrate ( $R_a$ ) was changed to 5.5, 8, and 20  $\mu\text{m}$ . Figure 13 shows the depth of dents formed as a function of substrate roughness. When the substrate roughness was low, solidification occurred inhomogeneously because of an uneven contact with the steel melt, thereby creating depressions and fine dents (Figures 12(a) and (b)). Since these depressions can result in surface cracking of the cast strips, it is desirable to maintain the high substrate roughness to promote homogeneous solidification of the solidified shell. However, the high substrate roughness is accompanied by deeper dent defects (Figures 12(c) and 13), which leads to

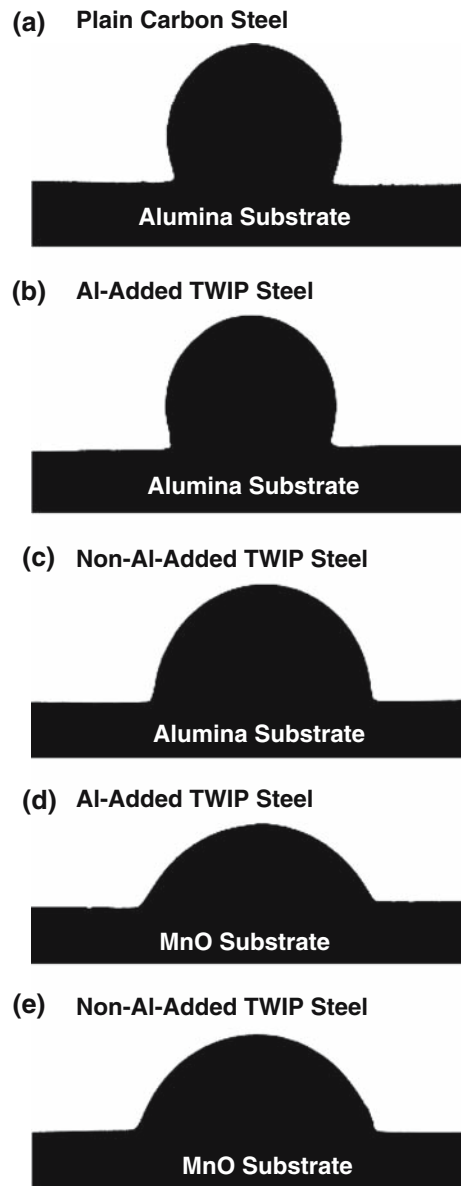


Fig. 9—Wetting behavior of the (a) plain carbon steel, (b) 1.5 wt pct Al-added TWIP steel, (c) non-Al-added TWIP steel on the alumina substrate, (d) 1.5 wt pct Al-added TWIP steel, and (e) non-Al-added TWIP steel on an MnO substrate. Wetting angles measured from the sessile drop method are 103, 95, 78, 57, and 67 deg for (a) through (e), respectively.

compromises that need to be made to choose the optimum surface roughness.

#### E. Effects of Chemical Composition of TWIP-Steel Melt

The development of dent defects was investigated by varying the Mn, Al, and C content in the steel (Figures 14(a) and (b)). Dents did not form in the steel without Mn but formed when the Mn content was greater than 15 wt pct (Figure 14(a)). The depth of the dent increased with increasing Mn content. The dent depth also increased with increasing Al content in the

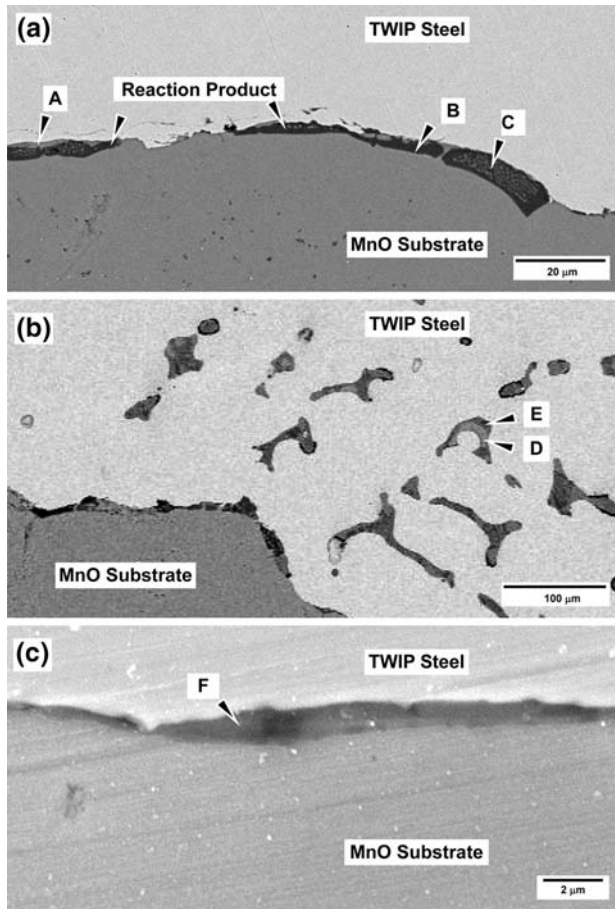


Fig. 10—SEM micrographs of the (a) and (b) 1.5 wt pct Al-added TWIP steel/MnO and (c) non-Al-added TWIP steel/MnO interfacial areas, showing various reaction products marked by A through F.

steel but was hardly affected by the C content in the steel (Figure 14(b)).

#### IV. DISCUSSION

The rapid-solidification experiments were conducted to understand and solve the problem of dent defects in strip-cast TWIP steels. According to the experimental data obtained, the influencing factors for the formation of dent defects include the oxide layer on the substrate surface, the substrate roughness, and Mn and Al content in the steel melt. As these factors are interrelated, they should be considered together to understand the formation mechanism of dent defects.

##### A. Dent-Formation Mechanisms of TWIP Steels

Dent defects formed on the strip-cast TWIP-steel surface (Figure 1) can be attributed to gases formed between the roll surface and the steel melt. The rapid-solidification experiments show that the dents are formed in the roughness valleys of the substrate, and the dent depth increases with increasing substrate roughness (Figure 8). This observation indicates that

Table I. Quantitative EDS Analysis Data of Reaction Products Present in the Interface between the MnO Substrate and the TWIP Steel (Atomic Percent)

Marked Area	Mn	Al	Si	Fe	O
A	40.6	6.1	—	1.8	51.5
B	15.7	27.5	—	—	56.9
C	23.3	21.3	—	—	55.3
D	32.2	1.6	10.6	—	55.7
E	15.5	26.9	—	0.8	56.7
F	32.4	5.1	5.4	3.2	54.0

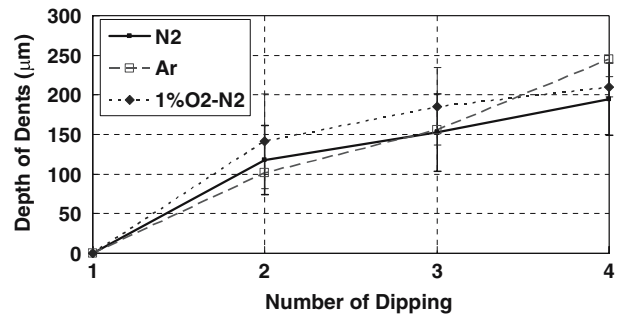


Fig. 11—Depth of dent defects as a function of atmosphere gas and number of dips.

dent formation is associated with gases formed between the substrate roughness and the solidified shell. Reasons for gas formation include the following: (1) decreased solubility of gases dissolved in the steel melt during solidification; (2) reaction between the oxide layer of the substrate surface and the steel melt; and (3) incomplete flow of the steel melt into the substrate roughness valleys and intrusion of atmosphere gases.

The gases present inside the steel melt include O, CO, N, and H. Considering that dents are formed even in the case of steel that has 1.5 wt pct Al, which will have extremely low oxygen of 5 ppm, oxygen does not seem to be related to the formation of dents. Since dents form in steels that do not contain carbon, dent formation is also not likely to be associated with the generation of CO (Figure 14(b)). The Mn in the steel is an element that raises the solubility of N, and the equilibrium solubility of N with 25 wt pct Mn is 1100 ppm. Considering that the N content in the steel melt is controlled to lower than 200 ppm, it can be predicted that nitrogen does not form during solidification. As for hydrogen, dents are formed irrespective of the hydrogen content between 5 and 20 ppm. Since the solubility of gases present in the steel melt is low in the solid state, the gases become segregated in the liquid phase during solidification and generally stay as pores at the end of solidification. They are thus not expected to cause dent formation on the surface of the solidified shells, and so the influence of gases present inside the steel melt on dent formation is small.

According to the MnO/TWIP-steel interfacial areas of Figure 10, Mn oxides react with the steel melt, but there are no pores formed as a result of gas reactions. Since dents develop even in steels that have no carbon, it is

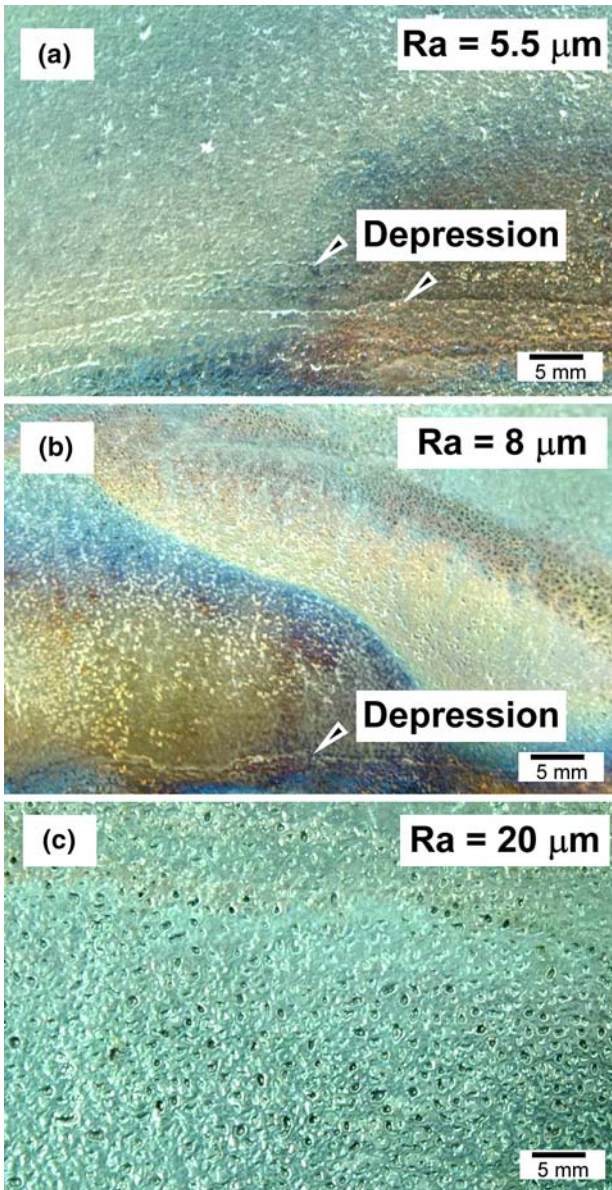


Fig. 12—Photographs of the surface of the solidified shells when the surface roughness ( $R_a$ ) of the substrate was (a)  $5.5\ \mu\text{m}$ , (b)  $8\ \mu\text{m}$ , and (c)  $20\ \mu\text{m}$  after the fourth dip.

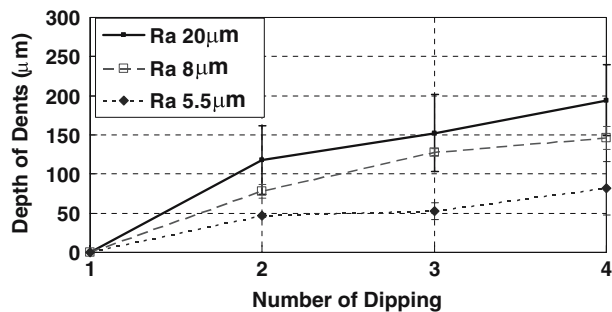


Fig. 13—Depth of dent defects as a function of surface roughness of the substrate and number of dips.

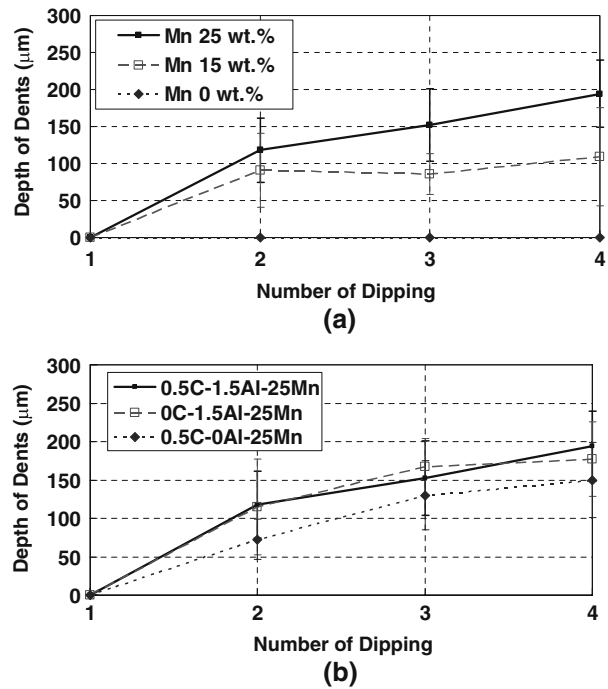


Fig. 14—Depth of dent defects as a function of number of dips showing the effect of (a) manganese and (b) carbon and aluminum in the TWIP-steel melt.

unlikely that gases are formed by a reaction between the oxide layer and the carbon in the steel melt.

Based on these observations, the formation of dents can be explained in a similar mechanism to that of air pockets formed on ribbon surfaces when atmosphere gases are introduced during melt spinning.<sup>[13,14]</sup> Since the rolls of the strip caster or the substrates used for rapid-solidification experiments have a high surface roughness, roughness valleys are not fully charged with the steel melt.<sup>[19–22]</sup> Solidification starts at the peaks of the roughness since the steel melt contacts those regions first. Since the roughness valleys are not fully charged with the steel melt because of insufficient fluidity as the temperature decreases, gas layers are formed in the roughness valleys. According to Gallois,<sup>[21]</sup> when a rough substrate contacts a steel melt, the charged depth of the steel melt is controlled by wetting angles, roughness curvature, and static pressure of the steel melt, while the roughness depth does not play any significant role. This implies that the depth of dents increases as the amount of gases introduced into the roughness valleys increases with increasing substrate roughness, when the roughness is made by using the same shot-blasting balls (*i.e.*, the same roughness curvature is obtained). When the roughness is processed by using blasting balls of 2 mm in diameter, the roughness dimples on the surface are approximately 1 mm in diameter, and the corresponding roughness depth is 0.13 mm. In the case of the first dipping, the surface roughness of solidified shells is approximately 0.05 mm, and the amount of atmosphere gases coexisting inside this roughness is approximately 0.03 cubic millimeters at room temperature, assuming a semispherical shape.



The oxides formed on the substrate surface are MnO and are formed either by the vaporization and sticking of Mn contained in the TWIP-steel melt onto the substrate surface or by the sticking of MnO formed on the surface of the steel melt onto the substrate surface.<sup>[20]</sup> The thickness increase of MnO on the substrate surface seems to be associated with an increase in the dent depth with an increasing number of dips and the fact that the Mn content inside the steel melt affects dent formation. According to the wetting-angle measurements of the TWIP-steel melt shown in Figures 9(b) through (e), the wettability of the TWIP steels is good and is particularly excellent in the case of the MnO substrate (Figures 9(d) and (e)). The improved wettability is a result of interfacial reactions whereby the wettability increases as reaction phases are formed on the interface in contact with the steel melt.<sup>[15,23,24]</sup>

The difference in the shape of the surface of the solidified shells that contact the roughness peaks in the first- and the fourth-dipped regions of Figure 8 can be explained by the wettability of the TWIP-steel melt with MnO of varying thickness. In other words, since the wettability between the steel melt and the oxide layer is good in the regions where oxide layers are present, the surface of the substrate roughness peaks become completely replicated by the steel melt. However, since the steel melt solidifies in the process of replicating the substrate surface, the gases become entrapped in the roughness valleys, and the steel melt does not enter there. The entrapped gases expand into the unsolidified areas and cause the dent defects. Since the wettability between roughness peaks and steel melt is poor in the case of a minor presence of MnO on the substrate surface, the roughness peaks are only in partial contact with the melt and are thus not totally replicated, as shown in Figure 8(b). This is explained by the fact that gaps are formed between the roughness peaks and the steel melt (or solidified shells) in this condition, and gases can flow between the substrate roughness and the solidified shells, leading to a liftoff phenomenon of the solidified shells from the substrate surface. When the gases are not sequestered, dent defects do not develop since there are no regions that allow the local gas to expand.

Gases entrapped in the roughness valleys expand by the heat of the steel melt and the latent heat during solidification, causing dent defects to occur. According to Wang *et al.*,<sup>[14]</sup> when the thickness of the gas layer is small (tens of  $\mu\text{m}$ ), the gases in contact with the steel melt are heated to a normal state within  $1\ \mu\text{s}$  and reach the average temperature of the steel melt and substrate. Assuming that the temperatures of the steel melt and substrate are  $1550\ ^\circ\text{C}$  and  $200\ ^\circ\text{C}$ , respectively, the gas temperature is calculated as  $875\ ^\circ\text{C}$ , which translated to an expansion of 3.8 times using the equation of state ( $PV = nRT$ ). The steel melt starts to solidify during volume expansion at the roughness peaks that are in direct contact with the steel melt, and, as a result, the gas expansion heads vertically in the direction of the nonsolidified roughness valleys of the substrate. A volume expansion of 3.8 times converts to a dent depth of  $0.35\ \text{mm}$  for a volume of a semispherical dent  $1\ \text{mm}$  in

diameter. This is similar to the dent depth observed in the strip casting and rapid solidification experiments. The depth of the dents increase as the oxide layer formed on the substrate surface increases the wettability between roughness peaks and steel melt, and the gases isolated in the roughness valleys move toward the steel melt.

### B. Preventative Methods of Dent Defects of TWIP Steels

The results of Section A require that the oxide layer on the substrate surface should be completely removed or that the thermal expansion of the gases be prevented to prevent the formation of dents. Hard brushing could be one method to remove the oxide layer of the substrate surface, to a level where no black manganese oxide is present on the rough substrate surface, especially in the case of steels with high-Mn content as in TWIP steels. However, since hard brushing can also damage the artificially processed roughness on the substrate surface, complete removal of the oxide layer from the substrate surface by brushing is not practical. If brushing is applied, it should be done to a point where the thickness of the oxide layer can be controlled and its homogeneity improved. Thus, in the present study, brushing was not used; instead, the shape of the substrate surface roughness was modified to prevent the formation of dents.

Figure 15(a) is a photograph of the substrate on which grid-type grooves  $0.35\text{-mm}$  wide,  $0.7\text{-mm}$  apart, and  $0.1\text{-mm}$  deep are made. The grooves are made narrow to prevent the steel melt from entering the grooves and thus enable the gases to flow in the groove valleys and escape through free interfaces. The rapid-solidification experiment was conducted on this substrate, and the surfaces of the solidified shells were photographed, as shown in Figures 15(b) and (c). The volume expansion of gases did not take place, and large dents were thus not formed on the surface of the solidified shells (Figure 15(c)), even after dipping the substrate ten times.

In the case of the roughness provided by shot blasting, the roughness peaks are sealed when they are contacted with the steel melt, which leads to volume expansion of the gases and consequently to the development of dent defects (Figures 4(b) through (d)). However, when narrow linear grooves are processed (Figure 15(a)), the expanded gases escape through the linear grooves. The horizontal plane between the linear grooves comes in direct contact with the steel melt (Figure 15(b)), and many of the fine dents are formed due to the formation of a fine surface roughness and consequent formation of oxides (Figure 15(b)). When a grid-type grooved substrate is used, not only do fine dents form between the linear grooves in the solidified shell, but it also shows an extremely fine solidification structure because the substrate is in direct contact with the steel melt. The solidified shell countering the linear groove section shows a coarse solidified structure, since the steel melt is not in contact with the substrate. This difference in the solidified structures can also cause a loss of surface reflectivity in the final strip product. While it is possible to introduce grid-type grooves on horizontal planes,

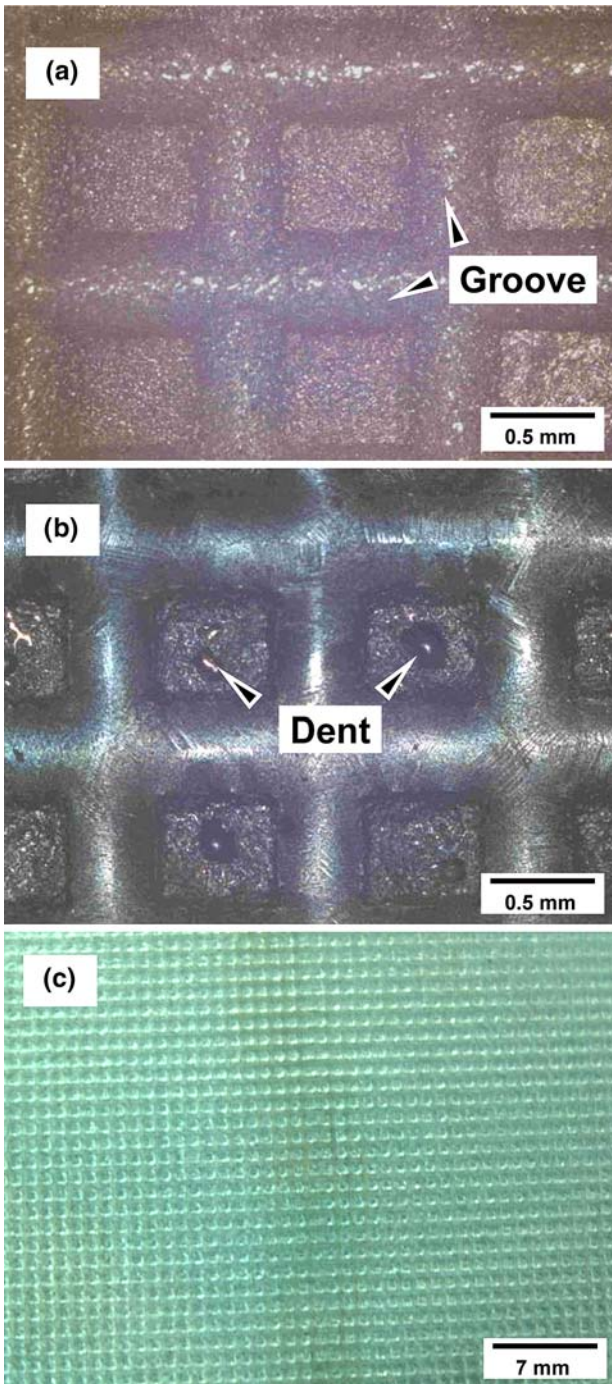


Fig. 15—Photographs of (a) grid-type grooved substrate, (b) the surface of the solidified shell, and (c) a low-magnification photograph of (b).

such as the substrates used for the rapid solidification experiments, they are not easily made on the curved roll surfaces of the strip caster.

Figure 16(a) is a photograph of the substrate on which longitudinal grooves were made along the dipping direction (along the roll revolving direction in the case of strip casting), and the roughness was provided by shot blasting. The rapid-solidification test was conducted on

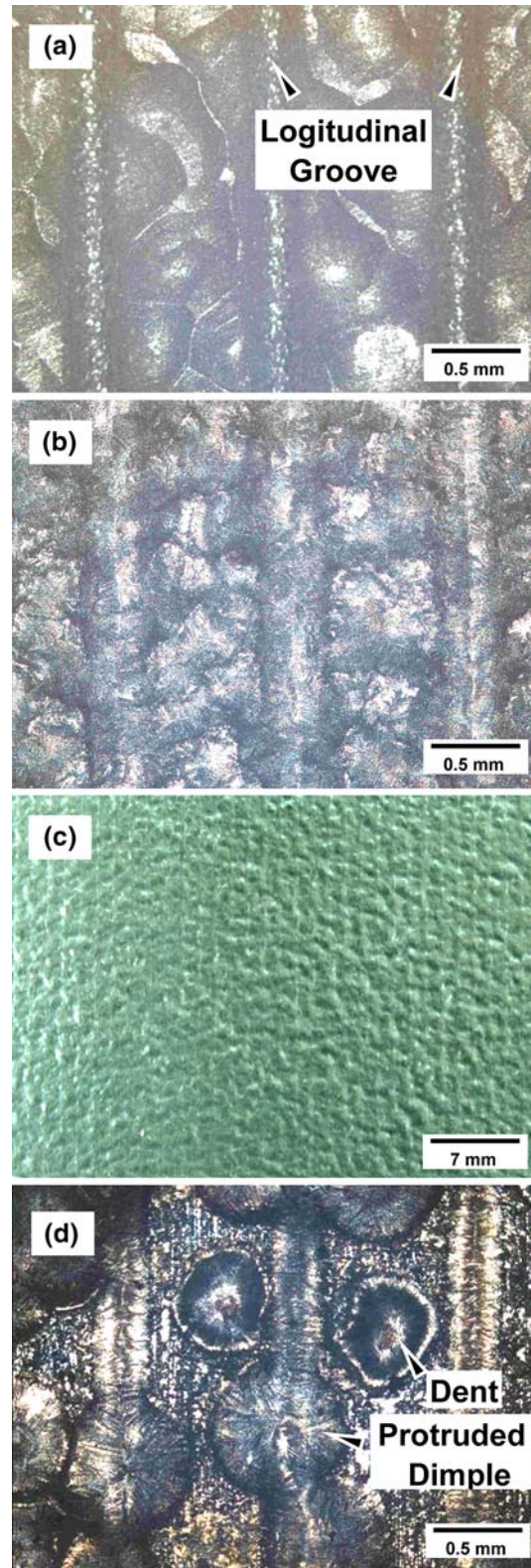


Fig. 16—Photographs of (a) longitudinal grooves and shot-blasting texture on the substrate, (b) the surface of the solidified shell, and (c) a low-magnification photograph of (b). (d) When the interval of the longitudinal grooves and the shot-blasting textured conditions are not appropriate, protruded dimples and dent defects around grooves are observed.

this substrate, and the photographs of the surface of solidified shells are shown in Figures 16(b) through (d). Since the molten steel cannot easily enter the longitudinal grooves, the gases can flow in these grooves and escape. In the case of the rolls in the strip caster, the gases would escape in this circumferential groove that is normal to the axis of the roll. Thus, large or fine dents will not form, and the surface of solidified shells will have a similar microstructure as the substrate on which only a shot-blasting roughness is provided, as shown in Figures 16(b) and (c). However, when the shot-blasting condition and the size of longitudinal grooves are not appropriate, protrusions of the solidified-shell surface are observed at the locations of the shot-blasting roughness in contact with the longitudinal grooves, while fine dents are formed at the roughness that is not in contact with the longitudinal grooves, as shown in Figure 16(d). The development of these dent defects is associated with the volume expansion of the gases at the roughness that is not in contact with the longitudinal grooves, whereas dent defects do not develop at the roughness in contact with longitudinal grooves because the expanded gases can escape through these grooves.

In the present study, the formation of dent defects during strip casting of TWIP steels was investigated and related to the volume expansion of gases and the solidification behavior of the steel. Based on the results, methods to predict and prevent dent formation are suggested. One approach is to provide longitudinal grooves on the substrate surface. Suppressing the volume expansion of gases is effective for preventing dents, and sound solidified shells, where even fine dents do not form, can be achieved by appropriately controlling the interval, width, and depth of the longitudinal grooves and the shot-blasting conditions, such as pressure, ball diameter, and ball material, all of which need to be optimized to allow the entrapped gases to escape.

## V. CONCLUSIONS

In this study, dent defects formed during strip casting of TWIP steels were analyzed by conducting simulation tests in a rapid-solidification apparatus. The following conclusions were obtained.

1. The roughness of the substrate surface, the oxide layer on the substrate surface, and the content of Mn and Al in the steel melt were the key factors controlling the formation of dent defects, while the composition of the atmosphere gases and the carbon content of the steel melt had no effect.
2. The interfacial reaction between the steel and the MnO formed from the Mn in the steel enhanced the wettability between the two, which brought the roughness peaks of the substrate surface in close contact with the steel melt and induced thermal expansion of gases into the steel melt, thereby leading to an increase in dent depth.
3. Dent formation was attributed to the entrapment of gases in the roughness valleys of the substrate

surface and to the volume expansion of gases heated by the high temperature of steel melt and latent heat during solidification. The depth of dents calculated by using the level of gas entrapped the gas temperature was similar to that of actual measurements.

4. The formation of dents could be prevented when the thermal expansion of gases was suppressed by making longitudinal grooves on the substrate surface that allowed the gases to escape. Sound solidified shells without dents could be obtained by optimizing the width and depth of longitudinal grooves and by controlling the shot-blasting conditions.

## ACKNOWLEDGMENTS

The authors thank POSCO and the National Research Laboratory Program (Grant No. M1040000361-06J0000-36110) funded by the Korea Science and Engineering Foundation (KOSEF) for the support of this work.

## REFERENCES

1. J.F. Grubb, D.B. Love, A. Murthy, and J.D. Nauman: *Proc. 69th Steelmaking Conf.*, Washington, DC, 1986, R.W. Stovall, ed., ISS, Warrendale, PA, 1986, vol. 69, pp. 841–47.
2. S. Miyake, F. Kogiku, M. Yumomoto, M. Ozawa, T. Kan, and A. Momoo: *Proc. Int. Symp. Casting of Near Net Shape Products*, Hawaii, HI, 1988, Y. Sahai, ed., TMS, Warrendale, PA, 1988, pp. 621–28.
3. T. Tohge, K. Amano, T. Maruyama, and M. Noda: *Int. Conf. New Smelting Reduction and Near Net Shape Casting Technologies for Steel*, Pohang, Korea, 1990, Korean Institute of Metals & Materials, Seoul, 1990, pp. 617–26.
4. W. Blejde, R. Mahapatra, and H. Fukase: *Iron Steelmaker*, 2001, vol. 28, pp. 43–48.
5. T. Bagsarian: *New Steel*, 2000, Dec., pp. 18–22.
6. I.D. Choi, D.M. Kim, S.J. Kim, D.M. Bruce, D.K. Matlok, and J.G. Speer: *Met. Mater. Int.*, 2006, vol. 12, pp. 13–20.
7. K.-W. Yi, Y.-T. Kim, and D.-Y. Kim: *Met. Mater. Int.*, 2007, vol. 13, pp. 223–28.
8. T.W. Kim and Y.G. Kim: *Mater. Sci. Eng., A*, 1993, vol. A160, pp. L13–L15.
9. G. Frommeyer, U.B. Brück, and P. Neumann: *ISIJ Int.*, 2003, vol. 43, pp. 438–46.
10. U. Brück, G. Frommeyer, O. Grässel, L.W. Meyer, and A. Weise: *Steel Res.*, 2002, vol. 73, pp. 294–98.
11. S.H. Park, I.S. Chung, and T.W. Kim: *Oxid. Met.*, 1998, vol. 49, pp. 349–71.
12. P.L. Ret, J.R. Brevick, and Y.K. Park: *Met. Mater. Int.*, 2007, vol. 13, pp. 285–93.
13. S.-C. Huang and C. Fiedler: *Metall. Mater. Trans. A*, 1981, vol. 12A, pp. 1107–12.
14. W.-K. Wang and C.-T. Kuo: *J. Mater. Sci.*, 1992, vol. 27, pp. 1440–44.
15. P.R. Chidambaram, G.R. Edwards, and D.L. Olson: *Metall. Mater. Trans. B*, 1992, vol. 23B, pp. 215–22.
16. K. Nakashima and K. Mori: *ISIJ Int.*, 1992, vol. 32, pp. 11–18.
17. D.A. Weirauch, Jr. and W.J. Krafick: *Metall. Mater. Trans. A*, 1990, vol. 21A, pp. 1745–51.
18. D.K. Choo, S. Lee, H.K. Moon, and T.W. Kang: *Metall. Mater. Trans. A*, 2001, vol. 32A, pp. 2249–58.
19. C.A. Muojekwu, I.V. Samarasekera, and J.K. Brimacombe: *Metall. Mater. Trans. B*, 1995, vol. 26B, pp. 361–82.

20. M.J. Ha, J.T. Choi, S.I. Jeong, H.K. Moon, S. Lee, and T.W. Kang: *Metall. Mater. Trans. A*, 2002, vol. 33A, pp. 1487–97.
21. B.M. Gallois: *J. Met.*, 1997, June, pp. 48–57.
22. D.Y. Lee: *Met. Mater. Int.*, 2006, vol. 12, pp. 153–60.
23. M.G. Nicholas: *Mater. Sci. Forum*, 1988, vol. 29, pp. 127–50.
24. P. Nolli and A.W. Cramb: *ICS Proc.*, Charlotte, NC, 2005, M.A. Baker, ed., Association for Iron and Steel Society, Warrendale, PA, 2005, pp. 357–68.